Mapping wildfire susceptibility area by using ArcGIS: A case study of the 2019-2020 Black Summer Fires in Kangaroo Island, South Australia

Hoan To[1], Yan Kiu Ko[1]

[1] Sustainable Infrastructure and Resource Management (SIRM), UniSA STEM, University of South Australia, Mawson Lakes, SA 5095, Australia

Correspondence: toydy004@mymail.unisa.edu.au; ORCID: 0009-0009-4417-2078

Abstract: The 2019-2020 bushfires season, Black Summer, is known as one of the worst seasons on record. Kangaroo Island (KI), located in South Australia, experienced severe devastation during this period. This study aimed to construct a bushfire susceptibility map for KI based on the 2019-20 Black Summer Fires event. Seven variables are selected for analysis: temperature, rainfall, aspect, slope, land use, land cover, and distance to road. Analytical hierarchy process (AHP) method is used to determine the weightings and ArcGIS software is used to perform raster analysis and produce a bushfire susceptibility map for KI. Results suggest that 39.1% and 58.7% of KI falls into the moderate, high-risk zones. Additionally, the western part of KI is more vulnerable to wildfire, especially in the Ravine des Casoars Wilderness Protection Park. The fire risk map produced provides valuable insights into the vulnerability of KI to bushfires, facilitating informed planning for future fire events.

Key words: Bushfires, GIS, mapping, AHP, weighted overlay, Kangaroo Island.

1. Introduction

Climate change has increased the magnitude, frequency, and extent of extreme climate events. With rising temperatures and changing precipitation patterns, climate change has contributed to longer fire seasons and drier soil and vegetation (US EPA 2016). Being the second driest continent on Earth, Australia has always been vulnerable to wildfire (Hiep et al. 2022). In 2019, Australia experienced the worst bushfire seasons in history, the 2019-2020 Black Summer bushfires season burnt over 5,000 hectares (ha) of landmass, claimed 173 lives and destroyed thousands of properties (Nur et al. 2023), (Nguyen, Merched & Stephen 2004).

Large-scale wildfire also brought huge threat towards wildlife. The 2019-20 fire burnt 21% of the native broadleaved forest in Australia, killed over 64000 koala and destroying millions of habitats. One of the most impacted species was the KI dunnart. Dunnart (*Sminthopsis aitkeni*) is an endangered species only found on KI (Department of Climate Change, Energy, the Environment and Water 2018). During the Black Summer fire, approximately 95% of their habitat is destroyed, and many were killed (Flannery 2020). The magnitude of damage wildfire caused reflects the need to study wildfire susceptibility and conduct fire mapping in vulnerable areas such as Kangaroo Island (KI). This can be helpful for planners and decision-makers to provide insights, establish fire protection strategies, and formulate policies to minimise impacts of fire on human, wildlife, and properties.

A bushfire susceptibility map could be a valuable resource to predict and manage the vulnerable bushfire area in the future (Hosseini & Lim 2021). Contributing factors for bushfire can be classified into four main categories: topography, meteorological, environmental, and anthropological factors (Nur et al. 2023), (He, Shirowzhan & Pettit 2022). Some studies pointed out that topographical factors, for example, namely elevation, slope, and aspect play a significant role in wildfire occurrence (Nikhil et al. 2021). Others emphasised the importance of human influences in bushfire accidents such as population density, housing density and distance from road (Lamat et al. 2021), (Clarke et al. 2019). He, Shirowzhan & Pettit (2022) found that several meteorological factors such as wind speed, and air temperature are the most important factors for magnitude and extent of bushfire. Fuel loads that belong to environmental factor is also suggested as another conditioning driver related to bushfire occurrence (Nur et al. 2023), (Tehrany et al. 2021). Lastly, Zhang, Lim & Sharples (2016) claimed that Normalised Difference Vegetation Index (NDVI) is the strongest predictive power for fire occurrence in South-Eastern Australia. Since various studies has shown different sets of factors identified as the most influential in bushfire occurrence in specific areas, it is crucial to determine what are the major factors that regulates bushfire at the study area (Hosseini & Lim 2021).

A literature review showed three common approaches for bushfire susceptibility mapping. Frequency Ratio (FR) is a simple statistical technique based on the relationship between the conditioning factors and the occurrence of bushfires. Hosseini & Lim (2021) used FR and other statistical models including Logistic Regression and Frequency Ratio (LRFR) and Gene Expression Programming Frequency Ratio (GEPFR) for bushfire mapping. These authors used the FR for their study resulting in around 80 to 90% accuracy. Another common approach for natural hazard prediction is Logistic Regression (LR). It is used to identify the spatial relationship between independent variable as bushfire occurrence and dependent variables as contributing factors (Zhang, Lim & Sharples 2016). Recently, machine learning (ML) algorithm has been widely applied in spatial predictions. Nur et al. (2023) used ML based on support vector regression to predict wildfires in Sydney, Australia. Lastly, the Analytic Hierarchy Process (AHP) method is also a popular choice for mapping wildfire susceptibility and prediction. AHP provides weighting of factors based on expert judgment and validate the weighting through consistency checks (Lamat et al. 2021); (Nikhil et al. 2021); (Naderpour, Rizeei & Ramezani 2021); (Tiwari, Mohammad & Dixit 2021). To judge the accuracy of the mappings, Lamat et al. (2021), Naderpour, Rizeei & Ramezani (2021), Hosseini & Lim (2021), and Tiwari, Mohammad & Dixit (2021) used receiver operating characteristics (ROC) and precision-recall curve (PRC), for validation of forest fire susceptibility map. Meanwhile, root mean square error (RMSE) is also a widely used method to quantify the bushfire models (Nur et al. 2023); (Naderpour, Rizeei & Ramezani 2021).

This study aimed to construct a bushfire susceptibility map for KI based on the 2019-20 Black Summer Fires event. In this research, a wildfire susceptibility map will be constructed based on factors collected from the 2019-20 Black Summer bushfire season in the KI. Seven contributing factors extracted based on expert opinions from nine articles. ArcGIS Pro 3.1.0 was used to perform data and mapping procession. The AHP approach was used to identify the weighting; and Root mean squared error (RMSE) method was deployed to check the accuracy of the susceptibility map.

2. Material and methods

2.1 Study area

KI (35.7752° S, 137.2142° E) is the third largest offshore island in Australia with an area of 4,405 square kilometres; KI is 112 km away from Adelaide, the capital city of South Australia (Bonney, He & Myint 2020). In Summer, the average high temperature is 24°C, whereas annual rainfall fluctuates at around 500mm, (Bonney, He & Myint 2020). It is a popular tourist spot renowned for its spectacular landscape and remarkable ecological value. KI houses over 890 native species, including endangered species such as KI Dunnart and Black-Cockatoo (Authentic KI n.d.). The island attracted over 150,000 visitors per annum, generating over AUD 180 million of revenue in 2021 (South Australian Tourism Commission 2021). Tourism also created a huge job market that supported the livelihood of locals, direct jobs on tourism accounted for 20% of total employment (Austrlian Trade Commission 2014).

The Black summer fire lasted for 6 weeks, from 20th December 2019 to 6th February 2020 (Liu, Freudenberger & Lim 2022). Almost half of this island (211,474 ha) was destroyed, most of the land burnt were from the two main reserves in KI: Flinders Chase National Park and Ravine des Casoars Wilderness Protected Area (Liu, Freudenberger & Lim 2022). Two lives were taken during the fire, with around 44,000 animals killed (Liu, Freudenberger & Lim 2022). KI had experienced severe wildfire in 2001 and 2007. Therefore, the recurring incidence of bushfires on KI illustrated the importance of wildfire susceptibility map in the study area.

2.2 Methodology and data

This study follows the methodological flowchart depicted in the Figure 1. To begin with, contributing factors of wildfire are identified through an initial round of literature review to determine the most frequently mentioned contributing factors and the classification intervals for each factor. After that, AHP models were built by relying on two point of views including Young Engineer and expert opinions. These AHP models was to assign appropriate weights to each factor. After formulating the weighting, a weighted overlay model was performed in ArcGIS to produce the susceptibility map. The result was compared with the fire severity map by Australian Google Earth Engine Burnt Area Map (AUS GEEBAM). This comparison is conducted to validate the accuracy of the susceptibility map and make any necessary adjustments to the assumptions and criteria used in the study.

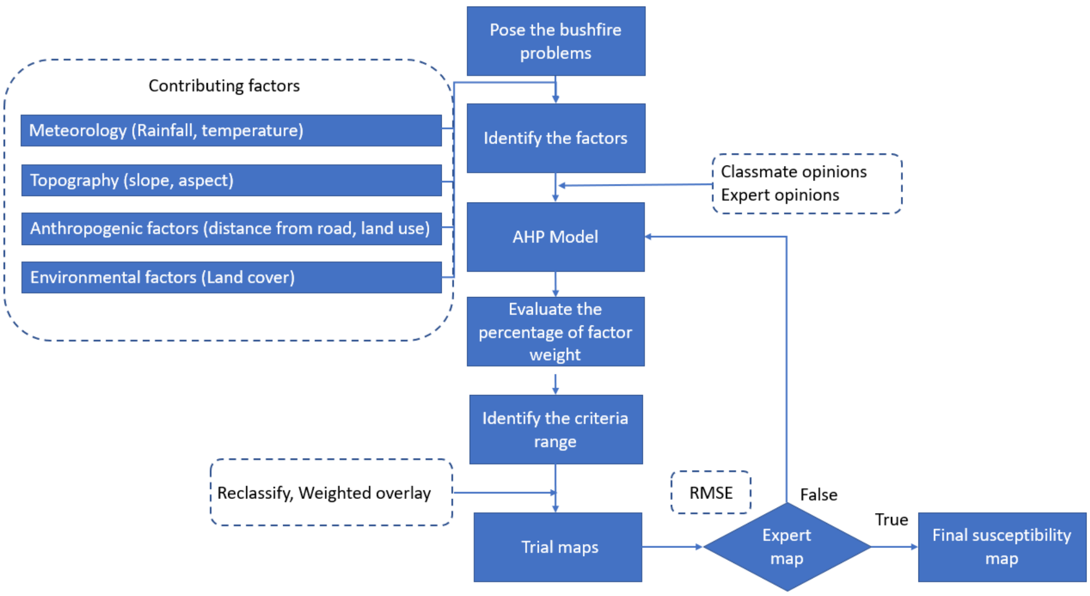

Figure 1: The flowchart of methodology in the research

2.2.1 Contributing factors

As various research has pointed out that the contributing factors for bushfire can be classified into topography, meteorological, environmental, and anthropological factors (Nur et al. 2023), (He, Shirowzhan & Pettit 2022). Hence the traditional literature-based approach is conducted to identify factors from these four main categories. Nine articles were selected to identify the main contributing factors, however, none of the articles were conducted in KI. To account for the influence of the local characteristics on factor selection, two studies about wildfire in KI. The elimination approach is adopted to select the contributing factors. All contributing factors discussed in each article is extracted, then only the influencing factors shared by four or more articles were selected. Seven factors selected are shown in Table 1.

Table 1: Bushfire causative factors

Bush fire causative categories	Bush fire causative criteria
Anthropogenic factors	Distance from road Land use
Environmental factors	Vegetation cover
Meteorological factors	Rainfall Temperature
Topological factors	Aspect Slope

Anthropogenic factors have effect on various aspect of fire such as fire extent, frequency, and seasonality (Lasslop & Kloster 2017). Human influences can be initiating fire and supressing fire directly; or indirectly by land use modification, forest fragmentation and changing vegetation composition (Lasslop & Kloster 2017). Distance from road can encourage wildfire occurrence and intensity, especially in tourist hotspots like KI. Sinha et al. (2023), Naderpour, Rizeei & Ramezani (2021), Naderpour, Rizeei & Ramezani (2021), and Tehrany et al. (2021) suggested that the passage of tourists can contribute to wildfire from fires set to clear forest paths, illegal dumping of cigarettes, cooking, campfires, and road repairs with coal tar burning. Secondly, the indirect anthropogenic factor of land use was also selected. Different land uses types had different flammability indexes. For instance, Bonney, He & Myint (2020) suggested that most fire ignites primarily on nature conserved lands or native forests, less than 5% initiates on agricultural or pastureland, whereas a large portion of landmass in KI were reserves or agricultural land uses.

For environmental factors, land cover is considered; land cover showed how vegetated the area is. Oxygen, heat, and fuel are the three crucial elements for a fire to sustain and spread. Vegetation serves as the fuel load of a fire. Additionally, Naderpour, Rizeei & Ramezani (2021), Naderpour, Rizeei & Ramezani (2021), and Hosseini & Lim (2021) ranked land cover as the most influencing factor in wildfires occurred in New South Wales and Victoria states.

Moving on to meteorological factors, higher temperature provides heat to the fire, increases the evapotranspiration rate, thereby increasing the flammability of the fuel load (vegetation) (Lamat et al. 2021). As for rainfall, Tiwari, Mohammad & Dixit (2021), Hosseini & Lim (2021) pointed out that rainfall affect the antecedent moisture level of the vegetation and soil, hence lower rainfall will contribute to a higher risk of wildfire occurrence.

Lastly, aspect and slope were the two main contributing factors identified in the topological category. Aspect is the facing of slopes, and the direction governs the intensity and duration of solar radiation received. Thereby in Southern hemisphere, north-facing slopes receives more solar radiation and generally have a higher temperature. Northward slopes are also characterised with drier vegetation with higher rate of evapotranspiration, hence favouring wildfire formation (Tehrany et al. 2021). Slope is another key influencer of wildfire as suggest by Naderpour, Rizeei & Ramezani (2021), Naderpour, Rizeei & Ramezani (2021), and Tehrany et al. (2021). It is proved that fire will spread faster and burn more severe on steep slope. For example, fire on a 20º slope spread 4 times faster than fire on a flat terrain (Lecina-Diaz, Alvarez & Retana 2014). Slope can also indirectly promote wildfire occurrences, through affecting vegetation cover, and climate elements like wind speed, precipitation, and temperature (Tehrany et al. 2021).

One way to quantify the influence of each criterion on bushfire is to rank the values with a common scale. In this study, a scale of 1 to 5 is used to represent very low, low, moderate, high, and very high influence on wildfire.

2.2.2 *GIS application tool*

Several geoprocessing tools were used to obtain the input data in the collecting data stage. The geographical data was derived from the Australian geographical data by using the *"Select by attribute"* and *"Make layer from selected feature"* tool. This boundary layer was used as a mask to extract other input raster data. The temperature and rainfall data in the study area was interpolated from mereological data of stations within study area by using the *"IDW method"*. *"Extract by mask"* tool was performed to obtain the land cover and land use data for KI. Land cover, for example, was separated into four raster shapefiles. Therefore, the *"Mosai to new raster"* tool was used to merge them into one raster data. Slope and aspect were derived with the *"Slope" and "Aspect"* tool in ArcGIS. Distance-to-road data was processed by using several tools, namely *Clip, Projection, Multiple Ring Buffer, and Extract by mask*. The *"Reclassify"* and *"Weighted overlay"* tool was used to build a susceptibility map. For calculating the map validation, we used *"Create random points" tool* to create 1000 points of interest across the Island. Finally, to identify the value of random points, we used the *"Extract multi values to points"* tool for map validation processes. The diagram of processing data was shown in the Figure 2.

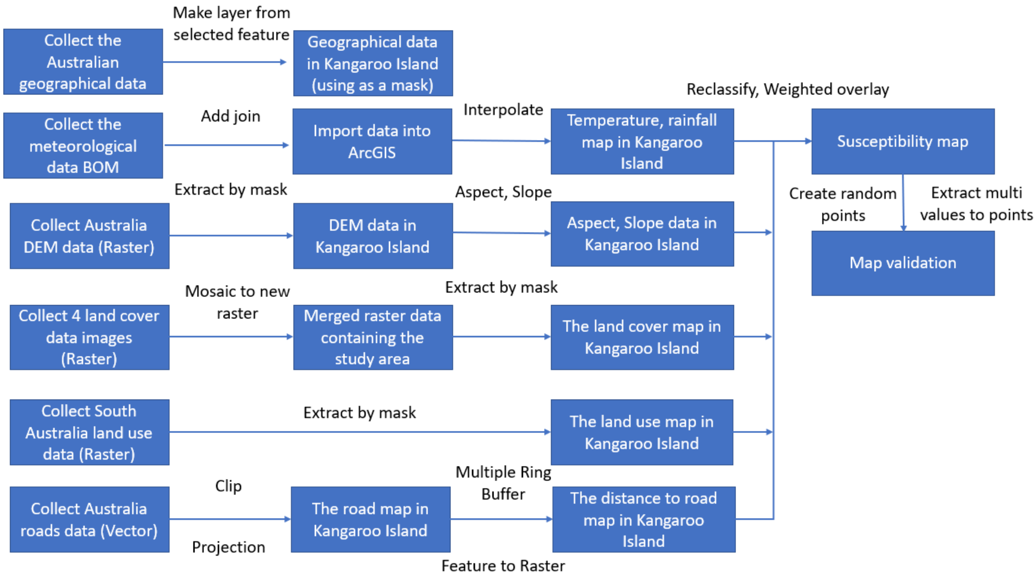

Figure 2: The diagram of obtaining input data by using the geoprocessing tool for the study.

2.2.3 *Fire severity map data*

The DPIE Remote Sensing and Landscape Science Branch of the Commonwealth Department of Agriculture, Water, and the Environment (DAWE) collaborated with the NSW Department of Planning, Industry and Environment (DPIE) to produce an Australian Google Earth Engine Burnt Area Map (AUS GEEBAM) based on Landsat 8 / Sentinel-2 imagery is used as a comparison map. This fire severity map showed fire intensity in 6 different classes: Unburnt, very low, Low and Moderate, High, and Very High severity. It was collected from DAWE website under environmental data.

2.2.4 Boundary data

The geographical data of KI is collected from Australian Statistical Geography Standard (ASGS) Edition 3 (released 7/2021), Australian Bureau of statistics. ASGS sub-classified Australia into a hierarchy of statistical areas for the publication and analysis of census and other data. The boundary of KI is used as a mask in processing raster input data for KI.

2.2.5 Topography data

Slope and aspect are derived from the elevation data by using 3 second SRTM Derived Digital Elevation Model (DEM) Version 1.0. The 3 second DEM was produced for use by government and the public under Creative Commons attribution and is used to derive topological data of slope and aspect.

The fuel load was more likely to dried on the steep slope than the mild slope; therefore, the steeper slope area is more vulnerable to fires (Lamat et al. 2021). In addition, the fires tend to move faster in a steeper slope than a gentle slope (Nikhil et al. 2021). The slope data in KI is comprised of 5 classes below. (1): 0-1.7^{o}; (2): 1.7-3.8^{o}; (3): 3.8-7.2^{o}; (4): 7.2-14.8^{o}; (5): 14.8-44.0^{o}.

Aspect is defined as the direction of slope, and it has a significant impact on vegetation cover and moisture in soil; this is because aspect controls the amount of solar radiation received on slopes (Tehrany et al. 2021). As the study area is in southern hemisphere, the northerly slope receives higher levels of solar radiation than south-facing slope (Zhang, Lim & Sharples 2016). Therefore, the fuels in north slope tend to dry sooner, making them easier to spark comparing to southernly slope. Slope into 5 classes as below. (5): 0-45^{o}; (3): 45-135^{o}; (1): 135-225^{o}; (3): 225-315^{o}; (5): 315-360^{o}

2.2.6 Meteorological data

The daily maximum temperature and total monthly rainfall data in December 2019 are obtained by accessing data at the Bureau of Meteorology (BOM) website, Australia Government. The study area, KI, contains 44 meteorological stations.

The rainfall data is only available in 13 meteorological stations. Data is interpolated with IDW to get the rainfall distribution. The rainfall map in the study area was shown in the Figure 3. Rainfall has an inverse relationship with the bushfire as less rainfall is associated with lower soil moisture content, and drier vegetation, increasing the risk of fires (Tiwari, Mohammad & Dixit 2021). The rainfall interval is divided into 5 categories by Natural breaks method (Jenks). Hence, the classification of the rainfall was shown as below. (5): 1.6-3.9 mm; (4): 3.9-5.7 mm; (3): 5.7-8 mm; (2): 8-10.8 mm; (1): 10.8-14 mm.

Temperature map is also created in a similar manner. Higher temperature has a positive influence on fire; heat increases evaporation rates, dries up fuels, and provides dry combustibles for bushfires (Tehrany et al. 2021); (He, Shirowzhan & Pettit 2022). Daily maximum temperature in December 2019 ranges from 38.0 to 42.3 ^{o}C. Based on the Natural breaks, we classified the temperature into five classes as follow. (1): 38.0-38.9 ^{o}C; (2): 38.9-39.9 ^{o}C; (3): 39.9-40.8 ^{o}C; (4): 40.8-41.6 ^{o}C, and (5): 41.6-42.3 ^{o}C.

2.2.7 *Environmental data*

The land cover data was collected from DEA's public data (DEA Land Cover (Landsat), Geoscience Australia Landsat Land Cover 25m). Digital Earth Australia (DEA) Land Cover translates over 30 years of satellite imagery into evidence of how Australia's land, vegetation and waterbodies have changed over time. The land cover data in study area consisted of four image data, including X5Y39, X5Y40, X4Y39, and X4Y40.

The classification for land cover data is based on the density of vegetation. Therefore, the higher the density, the higher the bushfire susceptibility level. Land cover is distributed into five classes. (5): Closed area (>65%); (4): open area (40 to 65%); (3): open area (15 to 40%); (2): sparse area (4 to 15%); and (1): scattered area (1 to 4%).

2.2.8 *Anthropogenic data*

The Catchment scale Land Use of Australia Map (CLUM) was used in this study. The dataset was updated in December 2020 and published by the Department of Agriculture (DA). The Statewide Road Network map on sealed and unsealed roads is provided by the Department for Infrastructure and Transport, Australia Government, and had been updated in May 2023. Hence navigable roads, including public and private access roads and tracks are included.

Land use data shows the type of vegetation. Conservation and natural environment areas have the highest wildfire occurrence (Nur et al. 2023). Furthermore, land uses such as urban area, infrastructure, cultivation areas, wetlands, and open water tends to stop the spread of bushfires (Nur et al. 2023). Therefore, the classification of land use data in KI was identified as below. (5): conservation and natural environment; (4): Production from dryland agriculture and plantations. (3): Production from irrigated agriculture and plantations; (2): Intensive uses; and (1): Water.

Distance to road is found to be one of the influencing anthropogenic factors (Zhang, Lim & Sharples 2016). In many cases, bushfire is sparked from tourist-incurred accident or fire crime (Nikhil et al. 2021). Thereby, bushfire risk increases with proximity to roads, and the classification is determined in five classes as follows. (5): 0-0.1 km, (4): 0.1-0.5 km; (3): 0.5-1 km; (2): 1-3 km; (1): 3-7 km.

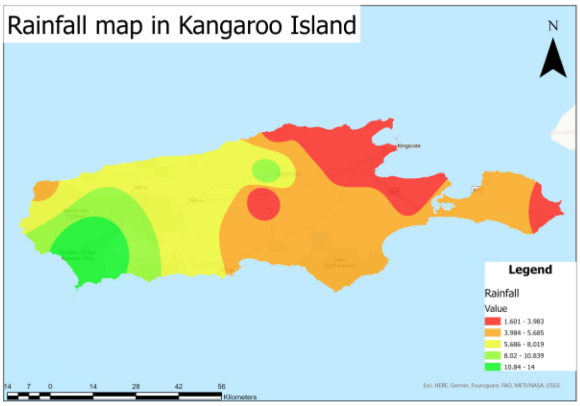

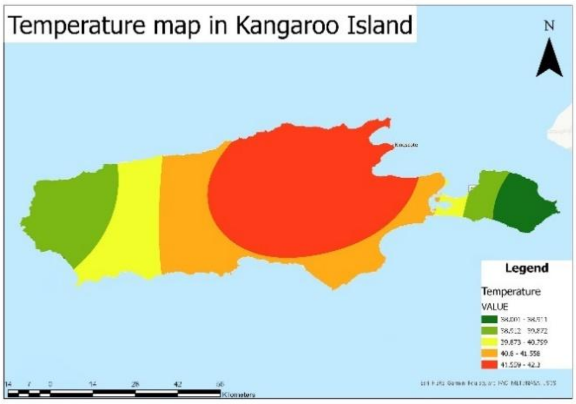

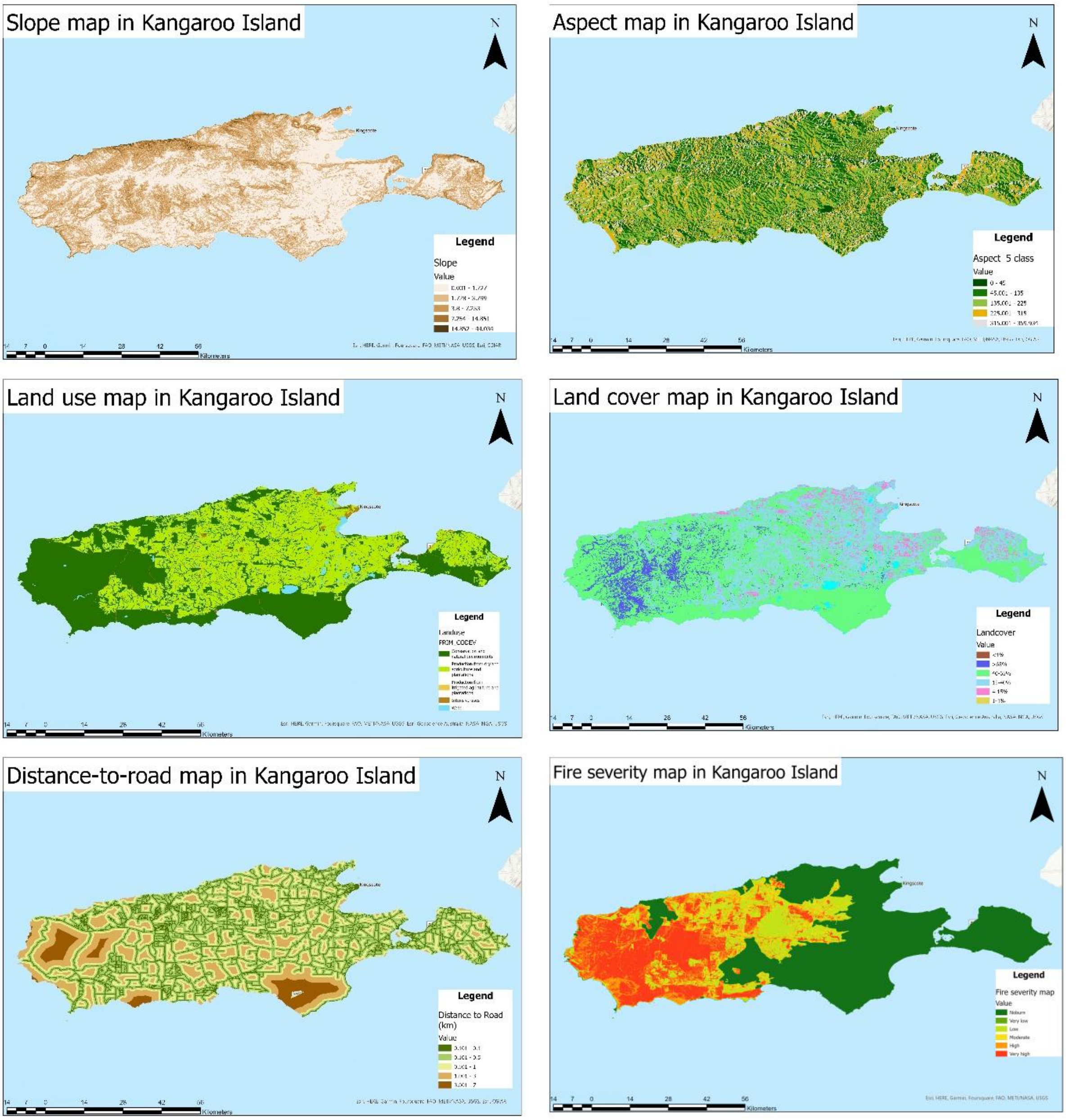

Figure 3: The contributing factor and bushfire severity map in the study area

2.2.9 AHP model

AHP is a multi-criteria decision technique that involves hierarchical structures to identify a problem based on experts' judgment (Lamat et al. 2021).

The AHP procedures involve four major steps, namely, constructing a matrix for pair-wise comparisons, calculating eigenvector (Vp) and weighting coefficient (Cp), calculating random index (RI), and validation of the model with the consistency ratio (CR) (Nikhil et al. 2021). Generally, a CR below 0.1 is acceptable (Naderpour, Rizeei & Ramezani 2021).

The principal eigenvalue (λ_{max}) is determined by using the equation: $\lambda_{\max} = \frac{1}{n} \sum_{Wti=1}^{n} \frac{(Cv)_i}{Wt_i}$

Where Wt_i defines weight for ranking, Cv represents the consistency vector and n symbolises total number of classes.

C_v is determined by multiplying pair-wise comparison matrix with the weight matrix. λ is computed by dividing the elements of Cv by corresponding weights.

$$Cv = \begin{bmatrix} a_{11} \times a_{12} \times \ldots \times a_{1n} \\ a_{21} \times a_{22} \times \ldots \times a_{2n} \\ \ldots \\ a_{n1} \times a_{n2} \times \ldots \times a_{nn} \end{bmatrix} \times \begin{bmatrix} W_{t1} \\ W_{t2} \\ \ldots \\ W_{tn} \end{bmatrix} \text{ or } Cv = a_{ij} \times Wt_i$$

where a_{ij} defines pair-wise comparison matrix in which a_{ij} = 1 and a_{ij} = 1/a_{ji}.
W_{ti} defines the weight value for ranking. Values of i and j ranges from 1 to n (number of criteria)

Consistency Index (CI) and Consistency Ratio (CR): $CI = \frac{\lambda_{\max} - n}{n-1}$; $CR = \frac{CI}{RI}$

Our research considered seven factors; the Random Index (RI) value is 1.32 as shown in Table 2.

Table 2: Random index (RI) for different number of criteria (n)

n	1	2	3	4	5	6	7	8	9	10
RI	0	0	0.58	0.9	1.12	1.24	**1.32**	1.41	1.45	1.49

2.2.10 Root mean squared error (RMSE)

Evaluating the model is a crucial step in understanding the prediction accuracy and reliability of it (Nur et al. 2023). RMSE compares the differences between the predicted model and the observed map and reflects the error of the model (Naderpour, Rizeei & Ramezani 2021). Hence a lower score is better.

$$RMSE = \sqrt{\frac{\sum_{i=1}^{n}(X_p - X_a)^2}{n}}$$

Where: n is the number of samples, X_p and X_a represents the predicted and actual value of the susceptibility map, respectively.

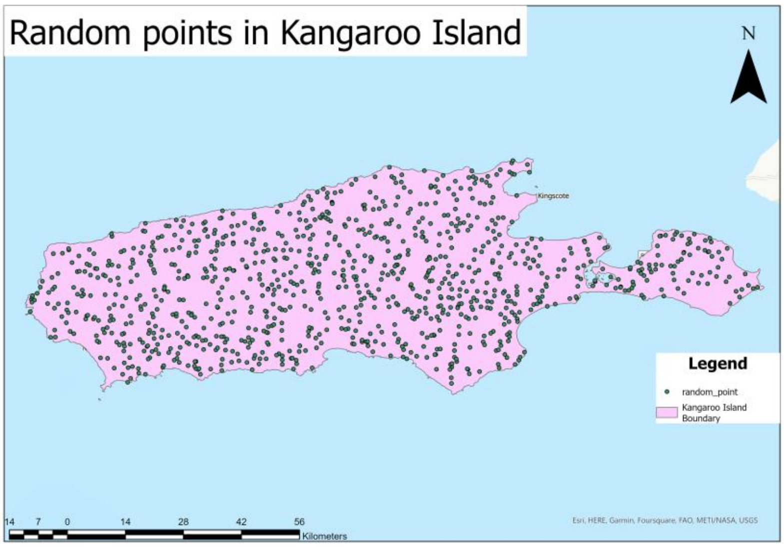

Figure 4: The 1000 random points in KI

In this research, we randomly choose 1000 points of interest in KI as in the Figure 4. By calculating the RMSE for 1000 points scattering the island, we derived the accuracy result of the predicted model.

3. Result

3.1 Evaluation of weighted percentage

Two trials were performed for assigning weightings to the contributing factors. Firstly, a dummy survey is used to obtain opinions from our fellow Young Engineers. Next, the traditional literature review approach is taken.

3.1.1 Young Engineer's views

A survey was conducted to respect the authenticity of the AHP method. Hence a questionnaire was sent out to our fellow Young Engineers to collect their opinions. A total of 15 responses were received and the weighting is presented in Table 6.

3.1.2 Experts' opinions

The articles used in identifying the contributing factors were used to conduct the desktop review. Rainfall and temperature consistently score less than other factors across the literatures (Nur et al. 2023) (Naderpour, Rizeei & Ramezani 2021), (Hosseini & Lim 2021), (Tehrany et al. 2021)**.** With consideration that only one-month data were collected, and the range is insignificant, meteorological factors were given a weighting of 3%. Aspect and slope both share a weighting of 10%. Although certain articles suggested that topological factors have a weak influence, the elevation of KI spanning from 0m to 300m, it also has landscape ranging from coastal cliff and plateau to sand dunes (Nur et al. 2023), (Naderpour, Rizeei & Ramezani 2021), (Hosseini & Lim 2021). The Kangaroo Island Landscape Board 2021). Thereby, the local topography is considered in adjusting the weighting. For anthropogenic factors, distance from road and land use are weighted as 10% and 27% respectively. Distance from road is adjusted considering KI being a tourist hotspot, whereas land use is considered as an influential factor in multiple articles (Nur et al. 2023)**,** (Tehrany et al. 2021), (Bonney, He & Myint 2020). Lastly, vegetation cover, the factor widely recognised as the most important contributor, has a weighting of 37%. The pairwise comparation and normalized weight matrix for AHP model were shown in the Table 3, Table 4, Table 5.

C1: Rainfall; C2: Temperature; C3: Slope; C4: Aspect; C5: Land use; C6: Land cover; C7: Distance to road.

Table 3: The pairwise comparation in contributing factors

	Young Engineer opinions							Expert opinions						
	C1	C2	C3	C4	C5	C6	C7	C1	C2	C3	C4	C5	C6	C7
C1	1.00	1.00	1.80	1.80	0.79	1.93	0.79	1.00	1.00	0.33	0.33	0.11	0.11	0.14
C2	1.00	1.00	1.80	1.80	0.79	1.93	0.79	1.00	1.00	0.33	0.33	0.11	0.11	0.14
C3	0.56	0.56	1.00	1.00	0.33	0.41	0.33	3.00	3.00	1.00	1.00	0.33	0.33	2.00
C4	0.56	0.56	1.00	1.00	0.33	0.41	0.33	3.00	3.00	1.00	1.00	0.33	0.33	2.00
C5	1.27	1.27	3.03	3.03	1.00	3.40	1.00	9.00	9.00	3.00	3.00	1.00	0.33	5.00
C6	0.52	0.52	2.44	2.44	0.29	1.00	3.40	9.00	9.00	3.00	3.00	3.00	1.00	7.00
C7	1.27	1.27	3.03	3.03	1.00	0.29	1.00	7.00	7.00	0.50	0.50	0.20	0.14	1.00
SUM	6.16	6.16	14.10	14.10	4.53	9.37	7.64	33.00	33.00	9.17	9.17	5.09	2.37	17.29

Table 4: Normalized weight matrix for AHP model by Young Engineers' opinions

Criteria	C1	C2	C3	C4	C5	C6	C7	Wti	SumCvi	λ
C1	0.16	0.16	0.13	0.13	0.17	0.21	0.10	0.15	1.18	7.75
C2	0.16	0.16	0.13	0.13	0.17	0.21	0.10	0.15	1.18	7.75
C3	0.09	0.09	0.07	0.07	0.07	0.04	0.04	0.07	0.50	7.32
C4	0.09	0.09	0.07	0.07	0.07	0.04	0.04	0.07	0.50	7.32
C5	0.21	0.21	0.21	0.21	0.22	0.36	0.13	0.22	1.75	7.87
C6	0.08	0.08	0.17	0.17	0.06	0.11	0.45	0.16	1.31	8.14
C7	0.21	0.21	0.21	0.21	0.22	0.03	0.13	0.17	1.25	7.13

λ_{max}= 7.61; Consistency index (CI)=0.1, Consistency Ratio (CR)=0.077

Table 5: Normalized weight matrix for AHP model by experts' opinions

Criteria	C1	C2	C3	C4	C5	C6	C7	Wti	SumCvi	λ
C1	0.03	0.03	0.04	0.04	0.02	0.05	0.01	0.03	0.21	7.10
C2	0.03	0.03	0.04	0.04	0.02	0.05	0.01	0.03	0.21	7.10
C3	0.09	0.09	0.11	0.11	0.07	0.14	0.12	0.10	0.80	7.71
C4	0.09	0.09	0.11	0.11	0.07	0.14	0.12	0.10	0.80	7.71
C5	0.27	0.27	0.33	0.33	0.20	0.14	0.29	0.26	2.04	7.81
C6	0.27	0.27	0.33	0.33	0.59	0.42	0.40	0.37	3.01	8.04
C7	0.21	0.21	0.05	0.05	0.04	0.06	0.06	0.10	0.73	7.38

λ_{max}= 7.55; Consistency index (CI)=0.09, Consistency Ratio (CR)=0.07

Table 6: The weighting result of factors from Young Engineer and experts

Contributing factors	**Unit**	**Class**	**Susceptibility class ranges and ratings**	**Susceptibility ratings**	**Weighting by Young Engineers (%)**	**Weighting by experts (%)**
Rainfall	mm	1.6-3.9 3.9-5.7 5.7-8 8-10.8 10.8-14	Very high High Moderate Low Very low	5 4 3 2 1	15	3
Temperature	Degree Celsius	38-38.9 38.9-39.9 39.9-40.8 40.8-41.6 41.6-42.3	Very low Low Moderate High Very high	1 2 3 4 5	15	3
Slope	degree	0-1.7 1.7-3.8 3.8-7.2 7.2-14.8 14.8-44.03	Very low Low Moderate High Very high	1 2 3 4 5	7	10
Aspect	degree	0-45 45-135 135-225 225-315 315-360	Very high moderate Low moderate Very high	5 3 1 3 5	7	10
Land use	-	Conservation and natural environments Production from dryland agriculture and plantations Production from irrigated agriculture and plantations	Very high High Moderate	5 4 3	22	27

		Intensive uses	Low	2		
		Water	Very low	1		
Land cover	%	10 (>65%)	Very high	5	17	37
		12 (40-65%)	High	4		
		13 (15-40%)	Moderate	3		
		15 (4-15%)	Low	2		
		16 (1-4%)	Very low	1		
Distance from road	km	<0.1 km	Very high	5	17	10
		0.1-0.5 km	High	4		
		0.5-1 km	Moderate	3		
		1-3 km	Low	2		
		3-7 km	Very low	1		

3.2 The bushfire susceptibility map

From the Young Engineers' perspective, the result showed that almost area of the island has the moderate and high susceptibility to bushfire. Product map indicates that there is a higher change of fire in the eastern and central part of the island. On the other hand, reserves at the west side including Ravine des Casoars Wilderness Protection and Cape Gantheaume Park were predicted to have the moderate-risk level (Figure 5). This is relatively different from the severity of official map where the area in the west of the island experienced the most serious level of bushfires. In addition, it was observed that wildfires almost had no influences on the plantation lands to the east of the island. Based on this evidence, the Young Engineers' opinion map showed the significant errors to the official map. That leads us to review the map result from the experts' opinions as below.

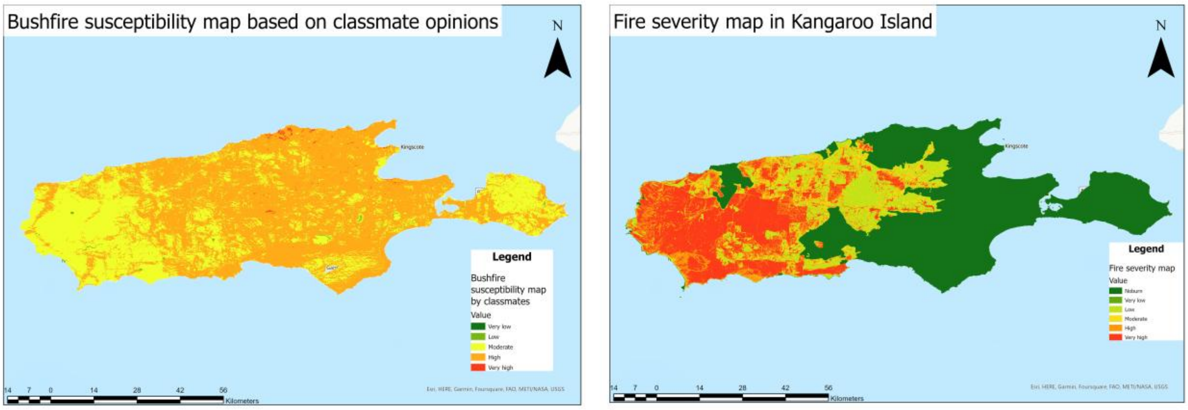

a. The bushfire susceptibility map based on Young Engineers' opinions.

b. The bushfire severity official map from DAWE

Figure 5: The bushfire susceptibility map based on Young Engineers' opinions.

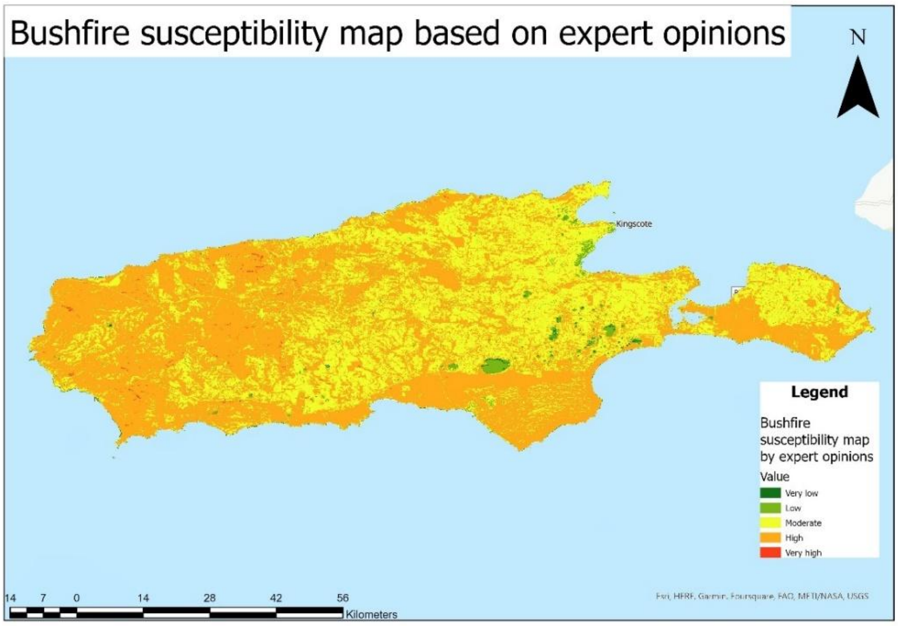

Figure 6: The bushfire susceptibility map based on expert opinions (literature review).

In expert opinions, the result showed that the high-risk level is concentrated in the western area such as the Ravine des Casoars Wilderness Protection Park. In addition, Cape Gantheaume, another conservation park located along the southern coast is also highly vulnerable (the orange-colour part). Meanwhile, plantation lands located in the middle of the island would have a moderate level of susceptibility to bushfires. There are only a few parts with the very high-risk level, but the amount of this area is rather insignificant. Although the result indicated that almost all area of the island had the moderate and high-risk susceptibility which is quite different from the official map, it showed a similar trend to the official map. That is the western area had the higher level of susceptibility than the area to the East. Therefore, we assumed that the result from experts' opinions is much more visually reliable than that from Young Engineer opinions.

Table 7: The result of mapping bushfires susceptibility area in risk extent.

	Susceptibility	Very low	Low	Moderate	High	Very high
By Young Engineers	Percentage (%)	0.0	0.3	37.1	62.4	0.3
By experts	Percentage (%)	0.4	1.7	39.1	58.7	0.2
Official map	Percentage (%)	0.0	12.5	6.8	9.9	21.5

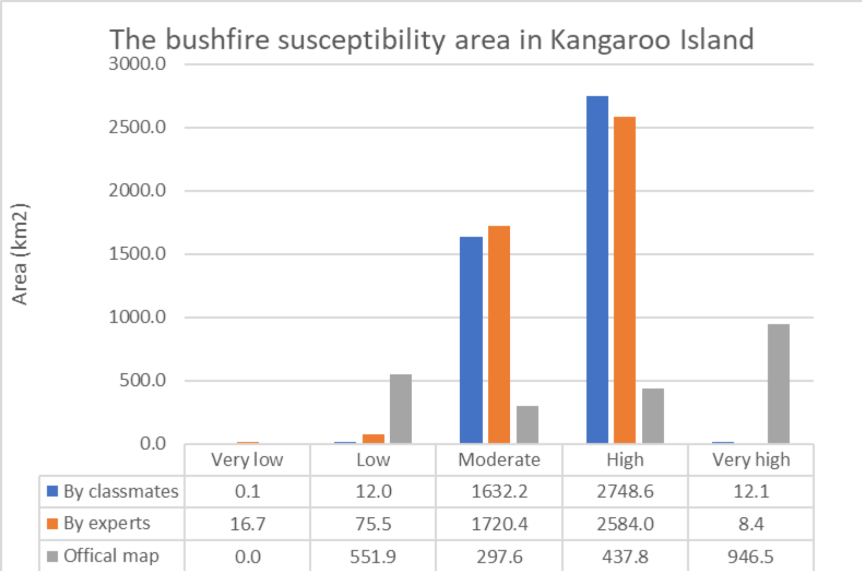

Figure 7: The bushfire susceptibility area in Kangaroo Island

As can be seen from the Figure 7 and Table 7, product maps from both trials show similar trend. Around 60% of the total land mass is under high risk of bushfire, while area with moderate risk made up for almost 40%, area under other risk levels account for only 1-2%. The result is different from the fire severity map by official department, where over 21% have experienced the highest level of fire severity.

3.3 Validation of the map

The RMSE result for validating map also supported our assumption. It showed that the RMSE value of the map from Young Engineer opinions is 2.167, which is bigger than that from expert's opinion (1.934). Although the difference between them is insignificant, it did show that our model was improved.

Table 8: The result of validation for the bushfires susceptibility maps

Weighting percentage (%)	Rainfall	Temperature	Slope	Aspect	Land use	Land cover	Distance from road	n	RMSE
By Young Engineers	15	15	7	7	22	17	17	1000	2.167
By experts	3	3	10	10	27	37	10	1000	1.934

3.4 The final susceptibility map

Based on side-by-side comparison, the susceptibility map based on experts' opinion shows a consistent trend with the official map. Area with the greatest bushfire risk is concentrated in the West side of KI, risk then decrease gradually towards the East. Whereas the higher risk area suggested by the weighting from Young Engineers is opposite with that from the official map. Additionally, RMSE results of the map by expert is lower than that by Young Engineer, thus suggesting that the weighting by expert can predict the bushfire susceptibility better. Therefore, the weighting derived from literature review will be the final susceptibility map presented in this study.

4. Discussion

As per the findings presented in the result section, the final map product exhibits certain similarities to the fire intensity map for KI. This shows that we found the correct trend for this problem and successfully incorporated influential factors related to bushfires in KI.

However, it is important to note that the area percentages do not align with the official map. We outlined several things that might contribute to the inconsistency. Firstly, the influencing factor candidates were the those most frequently mentioned in the articles we consulted. The small sampling size may lead to biased result, as fewer common factors could still play a significant role in our study area. Furthermore, none of the studies we referred to were specifically conducted in KI. These factors could potentially explain the disparities between the maps. Secondly, all classifications for scale data are done with natural breaks, while that for categorical data is done by using its original classification. This approach may have led to erroneous data classification and influenced the weighting assigned to each value and subsequently the scores allocated to each sample points.

In this study, we employed a simplified version of the AHP approach. AHP is a decision-making method that is simple, in a sense that it does not involve building any statistical model, using machine learning techniques or the use of statistical analytical software. Hence it is a flexible and simple tool. However, our results also suggested the importance of engaging a panel of experts as weighting results are entirely dependent on the perspectives and judgments of these individuals.

Several recommendations for further studies can be made based on the findings of this research. Firstly, a proper AHP can be conducted to understand the influencing factors for bushfire in KI, alternative methodologies beyond AHP should be explored to enhance the accuracy and robustness of bushfire risk mapping. Secondly, instead of focusing on a case study, the long-term wildfire trend and dynamics could be investigated through analysing all past wildfire events and future climate projections to construct a wildfire risk mapping.

There are several limitations in this study. Firstly, our temperature data was obtained by 4 stations having available temperature data. As a result, the interpolation result might be affected by the limited input data. We are only considering data in December 2019; therefore, data can be easily affected by outliers and is not representative. Secondly, factors are selected and classified based on personal interpretation on literature results, hence they may not be representative. Thirdly, AHP approach replies on judgment of participants to decide the weightings, hence it is inherently subjective and can be influenced by personal values, experience and biased. Additionally, we performed a dummy version of AHP, thus adding more uncertainty to the results. Furthermore, RMSE was used in this research to assess the accuracy of the susceptibility map. 1000 random points across the island only represent for 1000 cell values of the raster data, whereas the actual number of cells in raster data is extremely massive. Consequently, the RMSE was not able to measure the errors for the entire model. However, it did show how the model changed due to changing in percentages of factor weights. In the next study, it is advisable to try our model with different values of weightings. It helps reduce the RMSE and make the study more valuable.

5. Conclusion

The 2019-20 Black Summer Fires severely devasted the Kangaroo Island, exerting tremendous impacts on human, wildlife, and properties. This study aimed to produce a bushfire susceptibility map for this island and obtained several key elements. Firstly, the analysis from the literature review identified that there are seven contributing factors influencing the bushfires on Kangaroo Island namely temperature, rainfall, aspect, slope, land use, land cover, and distance to road. The result from Analytical hierarchy process (AHP) method suggested that land cover and land use were found as these most influential drivers causing bushfires in Kangaroo Island. Secondly, the bushfire susceptibility map result showed that 39.1% and 58.7% of the island falls into the moderate, high-risk zones. Moreover, the western part of KI is more vulnerable to wildfire, especially in the Ravine des Casoars Wilderness Protection Park. Although there is a difference between our result and the official severity map created by DAWE, our findings showed the similarities of the bushfire trend in this island, suggesting insights and fire protection strategies for authoritative organizations. Further studies need to be considered to get in-depth understanding and exam more accurately possible bushfires area in Kangaroo Island.

6. References

Australian Trade Commission 2014, *Kangaroo Island Tourism Employment Plan*, viewed 7 June 2023<https://www.austrade.gov.au/ArticleDocuments/5499/.>.

Authentic Kangaroo Island n.d., *Nature and Wildlife*, Kangaroo Island official website | Authentic Kangaroo Island, <https://authentickangarooisland.com.au/our-kangaroo-island/nature-and-wildlife/>.

Bonney, MT, He, Y & Myint, SW 2020, 'Contextualizing the 2019–2020 Kangaroo Island Bushfires: Quantifying Landscape-Level Influences on Past Severity and Recovery with Landsat and Google Earth Engine', *Remote Sensing*, vol. 12, no. 23, p. 3942.

CFS n.d., *SA Country Fire Service*, SA Country Fire Service, <https://www.cfs.sa.gov.au/about/about/bushfire-history/>.

Clarke, H, Gibson, R, Cirulis, B, Bradstock, RA & Penman, TD 2019, 'Developing and testing models of the drivers of anthropogenic and lightning-caused wildfire ignitions in south-eastern Australia', Journal of Environmental Management, vol. 235, pp. 34–41.

Department of Climate Change, Energy, the Environment and Water 2018, *Kangaroo Island dunnart - DCCEEW*, Dcceew.gov.au, viewed 6 June 2023 <https://www.dcceew.gov.au/environment/biodiversity/threatened/species>.

Flannery, T 2020, *Australia's 'black summer' bushfires showed the impact of human-wrought change | Tim Flannery*, the Guardian, <https://www.theguardian.com/environment/2020/jul/31/australias-black-summer-bushfires-showed-the-impact-of-human-wrought-change-aoe>.

He, W, Shirowzhan, S & Pettit, CJ 2022, 'GIS and Machine Learning for Analysing Influencing Factors of Bushfires Using 40-Year Spatio-Temporal Bushfire Data', *ISPRS International Journal of Geo-Information*, vol. 11, no. 6, p. 336.

Hiep, H, Merched, A, Stephen, W, Clutterbuck, H, Doyle, M, Webb Ware, J, … Pfeiffer, C 2022, 'The black summer bushfires: impacts and risk factors for livestock bushfire injury in south-eastern Australia', *Australian Veterinary Journal*, vol. 100, no. 7, pp. 306–317.

Hosseini, M & Lim, S 2021, 'Gene expression programming and ensemble methods for bushfire susceptibility mapping: a case study of Victoria, Australia', Geomatics, *Natural Hazards and Risk*, vol. 12, no. 1, pp. 2367–2386.

Lamat, R, Kumar, M, Kundu, A & Lal, D 2021, 'Forest fire risk mapping using analytical hierarchy process (AHP) and earth observation datasets: a case study in the mountainous terrain of Northeast

India', *SN Applied Sciences*, vol. 3, no. 4, p. 425.

Lasslop, G & Kloster, S 2017, 'Human impact on wildfires varies between regions and with vegetation productivity', *Environmental Research Letters*, vol. 12, no. 11, p. 115011.

Lecina-Diaz, J, Alvarez, A & Retana, J 2014, 'Extreme Fire Severity Patterns in Topographic, Convective and Wind-Driven Historical Wildfires of Mediterranean Pine Forests', in HYH Chen (ed.), *PLoS ONE*, vol. 9, no. 1, p. e85127.

Liu, J, Freudenberger, D & Lim, S 2022, 'Mapping burned areas and land-uses in Kangaroo Island using an object-based image classification framework and Landsat 8 Imagery from Google Earth Engine', *Geomatics, Natural Hazards and Risk*, vol. 13, no. 1, pp. 1867–1897.

Naderpour, M, Rizeei, HM & Ramezani, F 2021, 'Forest Fire Risk Prediction: A Spatial Deep Neural Network-Based Framework', *Remote Sensing*, vol. 13, no. 13, p. 2513.

Nguyen, H, Merched, A & Stephen, W 2004, 'The Summer 2019–2020 Wildfires in East Coast Australia and Their Impacts on Air Quality and Health in New South Wales, Australia', *International Journal of Environmental Research and Public Health*, vol. 1, no. 1, pp. 1–2.

Nikhil, S, Danumah, JH, Saha, S, Prasad, MK, Rajaneesh, A, Mammen, PC, … Kuriakose, SL 2021, 'Application of GIS and AHP Method in Forest Fire Risk Zone Mapping: a Study of the Parambikulam Tiger Reserve, Kerala, India', *Journal of Geovisualization and Spatial Analysis*, vol. 5, no. 1.

Nur, A, Kim, Y, Lee, J & Lee, C-W 2023, 'Spatial Prediction of Wildfire Susceptibility Using Hybrid Machine Learning Models Based on Support Vector Regression in Sydney, Australia', *Remote Sensing*, vol. 15, no. 3, p. 760.

Sinha, A, Suresh Nikhil, Ajin, RS, Jean Homian Danumah, Saha, S, Romulus Costache, … Abioui, M 2023, 'Wildfire Risk Zone Mapping in Contrasting Climatic Conditions: An Approach Employing AHP and F-AHP Models', vol. 6, no. 2, pp. 44–44.

South Australian Tourism Commission 2021, *Kangaroo Island Regional Profile*, viewed 7 June 2023< /https://tourism.sa.gov.au/media/hzlgcscr/kangaroo-island-regional-tourism-profile-march-2021.pdf>.

Tehrany, MS, Özener, H, Kalantar, B, Ueda, N, Habibi, MR, Shabani, Fariborz, … Shabani, F 2021, 'Application of an Ensemble Statistical Approach in Spatial Predictions of Bushfire Probability and Risk Mapping', in A Touhafi (ed.), *Journal of Sensors*, vol. 2021, pp. 1–31.

The Kangaroo Island Landscape Board 2021, *Kangaroo Island Landscape Plan 2021–2026*, viewed 8 June 2023 <https://cdn.environment.sa.gov.au/landscape/docs/ki/kangaroo-island-landscape-plan-21-26-final-print.pdf>.

Tiwari, A, Mohammad, S & Dixit, A 2021, 'GIS-based forest fire susceptibility modeling in Pauri Garhwal, India: a comparative assessment of frequency ratio, analytic hierarchy process and fuzzy modeling techniques', *Natural Hazards (Dordrecht)*, vol. 105(2), pp. 1189–1230.

US EPA, O 2016, *Climate Change Indicators: Wildfires*, www.epa.gov, viewed 6 June 2023<https://www.epa.gov/climate-indicators/ >.

Zhang, Y, Lim, S & Sharples, JJ 2016, 'Modelling spatial patterns of wildfire occurrence in South-Eastern Australia', Geomatics, *Natural Hazards and Risk*, vol. 7, no. 6, pp. 1800–1815.